

Lawrence Berkeley National Laboratory

Recent Work

Title

Textural Characterization and Its Applications on Zinc Electroplated Steels

Permalink

<https://escholarship.org/uc/item/2t86s0qz>

Authors

Shaffer, S.J.

Morris, J.W.

Wenk, H.R.

Publication Date

1990-05-01

Center for Advanced Materials

CAM

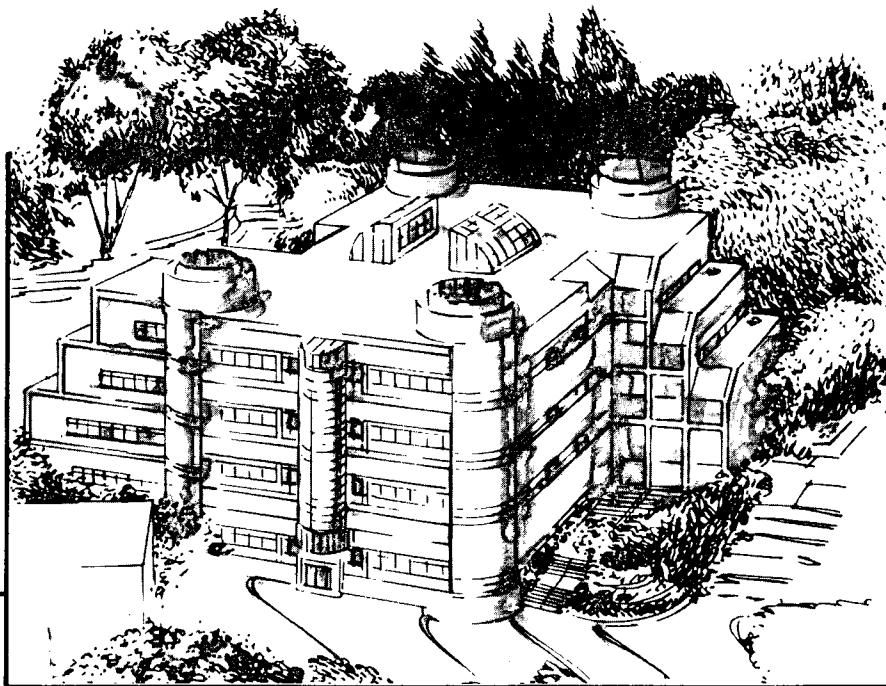
For Reference

Not to be taken from this room

To be presented at The Metallurgical Society
Annual Fall Conference, Detroit, MI,
October 5-7, 1990, and to be published
in the Proceedings

Textural Characterization and Its Applications on Zinc Electroplated Steels

S.J. Shaffer, J.W. Morris, Jr., and H.-R. Wenk



Materials and Chemical Sciences Division
Lawrence Berkeley Laboratory • University of California
ONE CYCLOTRON ROAD, BERKELEY, CA 94720 • (415) 486-4755

Prepared for the U.S. Department of Energy under Contract DE-AC03-76SF00098

Bldg. 50 Library.

Copy 1

LBL-29185

DISCLAIMER

This document was prepared as an account of work sponsored by the United States Government. While this document is believed to contain correct information, neither the United States Government nor any agency thereof, nor the Regents of the University of California, nor any of their employees, makes any warranty, express or implied, or assumes any legal responsibility for the accuracy, completeness, or usefulness of any information, apparatus, product, or process disclosed, or represents that its use would not infringe privately owned rights. Reference herein to any specific commercial product, process, or service by its trade name, trademark, manufacturer, or otherwise, does not necessarily constitute or imply its endorsement, recommendation, or favoring by the United States Government or any agency thereof, or the Regents of the University of California. The views and opinions of authors expressed herein do not necessarily state or reflect those of the United States Government or any agency thereof or the Regents of the University of California.

Textural Characterization and its Applications on Zinc Electroalvanized Steels

S. J. Shaffer, J.W. Morris, Jr. and H.-R. Wenk[†]

Center for Advanced Materials
Materials and Chemical Sciences Division
Lawrence Berkeley Laboratory
1 Cyclotron Road
Berkeley, CA 94720

and

Department of Materials Science and Mineral Engineering
University of California, Berkeley

[†]Department of Geology and Geophysics
University of California, Berkeley

May 1990

This work was supported by the Director, Office of Energy Research, Office of Basic Energy Science, Material Sciences Division of the U. S. Department of Energy under Contract No. DE-AC03-76SF00098 and by the Ford Motor Company, Rouge Steel Company, and LTV Steel Company.

Textural Characterization and its Applications on Zinc Electrogalvanized Steels

S. J. Shaffer, J.W. Morris, Jr. and H.-R. Wenk[†]

Center for Advanced Materials, Lawrence Berkeley Laboratory
1 Cyclotron Rd. Berkeley, CA, 94720

[†]Department of Geology and Geophysics, University of California, Berkeley, 94720

Methods of characterization and description of crystallographic texture in both laboratory prepared and commercial zinc electrogalvanized steel sheets are presented. Specific examples of simple in-plane normalization techniques, and pole figures obtained from deformation and friction studies are presented. Strong evolutions of texture are observed in friction testing. Coatings containing orientations which are unfavorable for slip show evidence of twinning and possibly recrystallization. The use of the complete orientation distribution function (ODF) is discussed with reference to deformation modelling studies and quantitative analysis of textural changes with depth. Other ODF applications include extraction of textural changes solely of the deformed surface layer resulting from friction testing as well as texture changes with coating thickness in as deposited coatings.

Introduction

Due to its hexagonal close-packed (hcp) crystal structure, zinc exhibits anisotropic properties. Additionally, electrochemical research has shown that strong preferred crystallographic orientations can be deliberately produced in electrogalvanized (EG) coatings⁽¹⁻⁵⁾. These sharp textures have effects on various aspects of performance, and it would be desirable to tailor the texture to the application for maximum performance.

It may seem obvious to metallurgists that the term texture refers to preferred crystallographic orientation in a polygranular sample, or in this case the zinc coating. However, the term texture has for some time also been used in reference to the surface roughness of a machined part or rolled sheet. This continues to lead to some confusion in discussions of automotive sheet products since both their surface roughness and preferred crystallographic orientation are of importance to their forming characteristics. For our purposes we shall reserve use of the word texture for the preferred distribution of grains (individual crystallites) having a particular crystallographic orientation with respect to a fixed reference frame; such as the sheet coordinates. Roughness or topography shall be used to refer to the surface topological feature distributions.

While the field of texture measurement and presentation is itself quite advanced, see for example Proceedings from recent ICOTOMs⁽⁶⁻⁸⁾, research on mechanistic understanding of the various behaviors of EG steels requires interdisciplinary communication between metallurgists, electrochemists, tribologists, and engineers. Following a review of some of the unanswered questions regarding texture in EG steels, this paper will provide some useful methods of such communication, followed by some example applications.

DIRECTIONS FOR TEXTURAL RESEARCH

While it has previously been reported that both its corrosion rate⁽⁹⁾ and paint adhesion performance⁽¹⁰⁾ depend on the crystallographic orientation of galvanized steels, in the area of formability of EG steels several questions remain unanswered.

To date one of the most variable and least predictable, hence least understood, characteristics of EG steels is their frictional behavior. Since the soft zinc surface is deformed during stamping as the sheet passes through drawbeads and under binders, one expects the texture to be influential. Indeed the work of Buckley⁽¹¹⁾ showed a dependence of friction on both crystal structure (fcc vs. hcp), and on orientation in hcp materials (0001 vs. $10\bar{1}0$). However the applicability of that high vacuum work to the present case is doubtful.

The frictional system involved in stamping EG steels comprises an entirely new, rather complex set of variables. A soft, highly textured zinc coating is deformed by rigid tooling in the presence of lubricant, while being constrained by the substrate steel sheet. The coated sheet possesses both surface roughness and microroughness, and undergoes bending, unbending, and sliding.

While some work has been published⁽¹¹⁾ and several new research programs are underway, the role and effect of zinc crystallographic orientation on friction in EG steels remains unclear, due in part to the absence of a suitable model. Several models of metallic friction make use of continuum plasticity⁽¹³⁻¹⁵⁾, however the extremely anisotropic and limited slip behavior of zinc, combined with the associated twinning propensity under certain loading conditions, causes the validity of these models to be questioned as well. Even the loading condition under which the zinc asperities are deformed is not well known.

While texture and deformation data have been reported on rolled bulk zinc⁽¹⁶⁾ and some as-electrodeposited structures^(1-5, 17), as yet no work has been reported regarding textural evolution in EG coatings due to stretching or frictional deformation. This information, combined with appropriate TEM analysis to identify the proper deformation mechanisms, is necessary for deformation modelling studies, which together, in turn, can help provide conceptual understanding to assist in developing more appropriate friction models.

Finally, texture changes with coating thickness have also been reported⁽¹⁸⁾, though not from the same sample. It is conceivable that design for optimum coating performance in pure zinc EG may include multilayer coatings, with the microstructure, including the texture of specific layers designed to meet individual applications. Specialized techniques are necessary in order to answer some of these questions as well.

Experimental Work

IN-SHEET-PLANE PERCENTAGE METHODS - (Assumes Fiber Texture)

Measurement

The relative intensities of x-ray reflections from a polygranular sample without any texture (random orientation) can be theoretically predicted and/or experimentally measured. Note that in the so-called "powder method", care should be taken to maintain the zinc powder in a reducing atmosphere. Powder samples of zinc generally have extensive oxide present which change the relative intensity ratios due to oxide peak overlap. Fine zinc filings, compacted by

Textural Characterization and its Applications on Zinc Electroplated Steels

isostatic compression (to prevent texture formation during compaction) can also be used. The measured values from the ASTM/JCPDS card #4-0831 can also be used. Alternatively the intensities may be calculated from crystal structure. See for example Cullity⁽¹⁹⁾ pages 107-143.

For non-random orientation distributions, these relative intensities are altered by the relative amounts of grains oriented with a particular plane parallel to the sheet. A commonly used and fairly rapid, simple technique for partial texture measurements makes use of normalization of measured intensities by the predicted intensities expected from a polygranular texture-free sample. An indication of the texture of the coating is obtained as follows:

Using a powder diffractometer (Cu K_{α} radiation was used in this work) with the sample in reflection geometry, a 2-theta scan is performed and the integrated intensities of several reflections is determined, these are termed I_{hkil} (where $hkil$ refers to the Miller-Bravais indices of the reflecting plane). Note that integrated intensities require background subtraction. Additionally for zinc coatings on steel, one must be careful using the $11\bar{2}2$ reflection (there is an overlap with the iron 211 peak) and that the $10\bar{1}3$ and $11\bar{2}0$ reflections are properly deconvoluted. Another caution is to exclude from the calculation higher order reflections such as 0004 , $20\bar{2}0$, $20\bar{2}2$, etc. which are multiples of 0002 , $10\bar{1}0$, $10\bar{1}1$ respectively and should have the same percentage. Each I_{hkil} is normalized by dividing it by its structure factor or "random" intensity, I^0_{hkil} , giving I^n_{hkil} . The values of I^0_{hkil} for zinc from the ASTM/JCPDS card for the 10 reflections used in this work are given in Table 1. The sum of these I^n_{hkil} is then computed, giving the total normalized intensity: I^n_{tot} . At this point one of two methods can be employed, however the results differ only by a scaling factor.

Table I X-ray Intensities for Normalization

<u>I/I_0</u>	<u>Reflection</u>
53	0002
40	$10\bar{1}0$
100	$10\bar{1}1$
28	$10\bar{1}2$
25	$10\bar{1}3$
21	$11\bar{2}0$
23	$11\bar{2}2$
17	$20\bar{2}1$
3	$10\bar{1}1$
8	$20\bar{2}3$

To obtain a "percentage of grains" with a particular orientation comparison, one divides each I^n_{hkil} by the I^n_{tot} and multiplies by 100. For a random distribution of orientations, each orientation would have the same percentage, equal to 100 divided by the number of reflections used in the calculation. For example 10% if 10 reflections are measured, and 12.5% if only 8 are used. This technique represents percentages of orientations *only from those reflections used in the calculations*. A limitation is that if too few peaks are used, the primary texture can be missed.

To obtain a "times random" comparison, one first divides I^n_{tot} by the number of reflections used in the calculation and uses this number to divide each I^n_{hkil} . Here, each

reflection from a zinc coating with no texture would have a value equal to 1, while a preference of grains with a particular plane parallel to the sheet surface would have a value greater than one. Similarly an orientation "less than random" would have a value less than one. This may have a more physical appeal, but again the values are representative of only those reflections measured.

Representation

For facilitating physical interpretation, the results are presented in a column chart with the orientations progressing from left to right, from basal through low angle pyramid, high angle pyramid, to the two prism planes, as shown schematically in Figure 1. Applications for this technique include quick surveying of both commercial and experimentally deposited coatings as well as an indicator of the consistency of the production line characteristics.

Using this technique, experimentally deposited laboratory coatings made using a cylindrical rotating cathode simulator, were surveyed. Several with very sharp in-sheet-plane textures were chosen for friction studies, four of which are shown in Fig. 2, along with schematic illustrations of zinc crystals corresponding to these orientations.

Limitations

Due to the geometry of a 2-theta scan, the above technique gives only an indication of a preference of grain orientations with a particular plane parallel to the sheet surface, without information about rotational distributions. Results of this technique therefore assume a fiber texture, or radial symmetry about the sheet normal (represented by the angle ψ in this work). For applications such as paint adhesion and corrosion resistance, this knowledge may be sufficient. In deformation modelling work however, calculations of resolved shear stresses (RSS), strains, and grain rotations depend not only on the orientation of the basal planes with respect to the sheet, but on the orientation of the a-axes about the c-axis, as well as the rotational distribution of the grains about ψ (Fig. 3).

POLE FIGURES

For more accurate modelling of deformation behavior in EG coatings, including surface friction, one needs more complete knowledge of the distribution of orientations. This can be obtained by measuring the 3-D distribution of a particular plane over the specimen using the Schultz⁽²⁰⁾ reflection technique and a three axis goniometer. In this work a Scintag/Nonius pole figure goniometer and Fe K_{α} radiation was used.

Results of these measurements are typically displayed in a pole figure, as the distribution of the "poles" (normals to the plane) in stereographic projection, either equal angle or equal area, with the sheet coordinates as the reference frame. Good descriptions of this technique can be found, for example, in the texts by Wenk⁽²¹⁾ or Hatherly and Hutchinson⁽²²⁾. The geometry of measurement and representation are shown in figure 4. All projections presented in this work are equal area projections.

It must be noted that the accuracy of this technique drops off beyond about 80 degrees from normal ($\chi < 10^{\circ}$). Hence, depending on the texture and symmetry, measurement of the distribution of other poles is sometimes necessary. For this work we measured the 0002, $10\bar{1}0$, $10\bar{1}1$, and $10\bar{1}2$ poles. We will later obtain the fully 3-dimensional orientation distribution functions (ODFs) for quantitative representation and modelling work.

Results and Discussion of Example Applications

BULK COATING DEFORMATION IN TENSION

Basal and prismatic pole figures, Fig. 5, shows the change in texture of two commercial zinc electrodeposits after 25% uniform tensile elongation. The deposit in Figure 5a shows very little change in texture after deformation, while that in 5b exhibits an evolution of the basal planes both away from the tensile axis (lower pole density along the North/South line) and towards the sheet normal (poles closer to the center of the circle).

SEM micrographs of the as deposited surface and surfaces after tensile straining provide the reason for the lack of change texture in coating #1 (Fig. 6). Straining was primarily accommodated by intergranular cracking, while in sample #2 slip and rotation of grains resulted in the change in topography. Some "orange peel" effect can also be seen due to rotation of the substrate ferrite grains. This may have significance in reference to drawbead simulator (DBS) friction testing where the tensile strains due to bending over the first shoulder would induce a change in the initial surface roughness, hence contact area, prior to contact with the second bead. This effect has been shown by Nine^(23,24) in work on bare steel and aluminum.

It is not clear whether the intergranular fracture during tensile elongation of commercial electrodeposit #1 should be expected or not. Research by Pak and co-workers⁽²⁵⁾ found cracking in commercial coatings exhibiting a majority of basal planes nearly perpendicular (85 degrees or more) to the sheet plane, and little cracking in those with pyramidal orientations (basal planes 40 to 70 degrees inclined to the sheet). The majority of planes in the present case appear to be a borderline case, mostly of 55 to 75 degree inclination and nearly fiber texture, mixed with lower tilt angles.

Cracking in zinc coatings may depend not only on the overall texture with respect to macroscopic stress or strain state, but also on the local grain to grain misorientation, and the inherent grain boundary strength. Even at favorable inclinations to the sheet plane, cracking might be expected for clusters of grains whose basal planes were oriented parallel to the loading direction (i.e. with their poles anywhere along the equator). Such groups of grains would have zero RSS on the basal slip system, thus strain accommodation in these regions would have to be through cracking. However, since twinning in zinc may be expected to occur under tension parallel to the basal planes for such grains, it is also possible that the deposition conditions of this particular coating led to inherently weak grain boundaries. Local texture measurements of grain misorientations across the fracture boundaries via TEM may be necessary to answer these questions.

FRICION TESTS

In friction testing the coating is deformed through loading applied at the surface. In drawbead simulation (DBS) friction testing, there are additional superimposed tensile and compressive strains on the coating due to bending and unbending of the sheet around the drawbeads. A description of the DBS test can be found in the publications by Nine⁽²⁶⁾.

Textural changes resulting from friction tests using a drawbead simulator are shown via the basal pole figures in Fig. 7 for two commercial coatings and three laboratory deposited coatings of widely differing textures. All coatings show movement of the basal poles opposite to

the drawing direction. This corresponds to the macroscopic direction in which the surface asperities would be pushed or sheared by the tooling.

In all of these figures there is also a reduction in intensity along the N/S line as was seen in the commercial tensile elongation specimen #2, which may be due to the superimposed tensile strain due to bending of the sheet around the drawbead. However, the redistribution of the basal poles is asymmetric, probably due to the sliding contribution of the surface loading. This asymmetry is particularly dramatic in laboratory samples (d) and (e).

It is also observed that a decrease in basal poles inclined "into" the loading direction took place. A surprising exception to this is the appearance of basal poles at about 45° "into" the loading direction in laboratory sample (c). Given the direction of macroscopic shearing, evolution of grains into this orientation from the original distribution via slip is not possible. One possible explanation is that these grains (or portions thereof) initially twinned due to compressive loading, thus transforming their original c-axes from the center of the pole figure to near the edge (The twin plane in zinc is $\{10\bar{1}2\}$. The c/a ratio of 1.856 gives rise to a 47° incline of this plane to the basal plane. Thus the c-axis of a twin in zinc lies 86° from that of the c-axis in the parent grain.) Subsequent grain rotation via slip may then have produced these inclined basal planes observed in the pole figure.

In laboratory sample (e), of strong near $11\bar{2}0$ prism orientation, obtained by adding cadmium to the electrolyte, the basal poles were seen to have moved to an orientation with no apparent connection to the original. As can be seen from the plot of RSS vs. α (Fig. 3c), a single crystal in the geometry corresponding to this sample would be unfavorably oriented for slip on the basal system under nearly any assumed loading condition ranging from shear to compression, hence one would expect either non-basal slip or twinning to take place.

Prismatic slip $\{10\bar{1}0\}\langle 11\bar{2}0\rangle$, which has been observed only at elevated temperatures in zinc would not lead to rotation of the basal planes to the final texture. Although the alternative slip system $\{11\bar{2}2\}\langle 11\bar{2}3\rangle$ (CRSS from 30 to 50 times higher than basal slip⁽²⁷⁾) could lead to rotation of the basal planes, it is much more likely that twinning took place. In fact the geometrical relationship of one twin variant to the original texture lies nearly exactly in the peak of the deformed texture. The same geometrical twinning relationship is consistent with the results in laboratory sample (d).

In addition to apparent twinning in the case of grains whose c-axes are inclined near the N/S direction in projection, there is a definite tendency towards a similar final texture. Due to the relatively low melting point in zinc, there is a strong possibility that the highly deformed surface layers were recrystallized, and that what we are observing is the superposition of similar recrystallized (and/or twinned) surface textures upon the original bulk coating texture. A technique for separation of this "composite" structure is necessary. Additionally, cross sectional TEM of the surface layer may help answer these questions.

ANALYSIS OF SURFACE LAYERS

From cross sectional observations the apparent depth of deformation of the zinc due to friction is surprisingly shallow, less than one micron (Fig. 8). Radiation from a copper target x-ray tube has considerable penetration power in zinc compared to the coating thickness, as also do x-rays from softer tubes such as iron, chromium or titanium (Fig. 9). Hence analysis of changes

Textural Characterization and its Applications on Zinc Electroplated Steels

in texture of the top 0.5 μm are confounded by signal from the bulk material using these radiation sources. To limit the signal to the volume of interest, one would require an extremely soft source of x-rays, such as the use of synchrotron radiation, or a different technique. One alternative technique, in which the surface layers are chemically removed, via a 10 to 15 second immersion using a 3% HNO_3 in distilled H_2O solution, is under development .

The basal pole figures in Fig. 10 are from an identical sample to laboratory #3 above, except that a straight strip-draw friction test was performed instead of the drawbead simulation. As such the coating was not subjected to any bending and unbending (hence no tensile stresses) and the coating deformation was entirely due to surface contact sliding. For this test a 9.5mm diameter cylindrical bead (same diameter as used in DBS test) with a nominal load of 750 lbs, over a 38mm strip width was used.

Qualitative Analysis

After chemical removal of 4 μm of coating, the measured texture reverts to the original. Comparison with the signal penetration from the Fe x-ray tube in Fig. 9 suggests that the depth of deformation due to twinning is more extensive than that observed in cross-section at the surface.

Quantitative Analysis

While comparison of the pole figures from different levels after etching allows one to qualitatively observe the changes in texture with depth, analysis of changes which are less dramatic than the above example become more difficult. In principle, with proper ODF computation and normalization procedures, one can subtract the "surface removed" texture from the "full thickness" texture and obtain the texture solely from the removed layer. Hence etching times can be reduced such that one micron at a time or less can be removed. This information can then be used for modelling studies of surface friction. This work is currently in progress.

Another application for this technique is for the determination of changes in texture with thickness on a single sample.

Conclusions

- 1) The In-Sheet-Plane method is good for a quick survey. If correlations with deformation are available, this method can give a prediction of cracking.
- 2) Pole figures and ODF's are necessary for deformation modelling studies.
- 3) Evidence that both basal poles inclined into loading and N/S inclined basal poles undergo twinning during friction testing. TEM studies are necessary to confirm and obtain volume fraction of twinning, as well as the extent of recrystallization, if any.
- 4) Surface removal techniques combined with ODF analysis are necessary for quantifying textural changes with thickness.

References

1. I. Tomov, et.al., "Factors influencing the preferential orientations in zinc coatings electrodeposited from chloride baths", *J. Appl. Electrochemistry*, v.19, pp377-382, (1989).
2. R. Sato, Crystal Growth of Electrodeposited Zinc: an Electron Diffraction and Electron Microscopic Study, *J. Electrochem. Soc.*, v.106, No.3, pp206-211, (1959).
3. D. J. Robinson & T. J. O'Keefe, On the Effects of Antimony and Glue on Zinc Electrocrystallization Behavior, *J. Appl. Electrochem.*, Vol. 6, No. 1, (1976).
4. D. J. Mackinnon, J.M. Brannen, & R.C. Kerby, The Effect of Cadmium on Zinc Deposit Structures Obtained from High Purity Industrial Acid Sulphate Electrolyte, *J. Appl. Electrochem.*, Vol. 9, No.1 (1979).
5. A. Weymeersch, et. al., "Zinc Electrodeposition at High Current Densities", *Plating and Surface Finishing*, (May 1981)
6. Proc. 8th ICOTOM, J.S. Kallend & G. Gottstein, eds., Santa Fe, NM, (1987).
7. Proc. 7th ICOTOM, C.M. Brakman , P. Jongenburger, & E.J. Mittemeijer, eds. Noordwijkhout, Netherlands, (1984)
8. Proc. 6th ICOTOM, S. Nagashima, ed. Tokyo, Japan, (1981).
9. Cited in ref (18), p217.
10. H. Leidheiser, Jr. and D.K. Kim, "Crystallographic Factors Affecting the Adherence of Paint to Deformed Galvanized Steels", *J. of Metals*, pp19-25, (Nov. 1976).
11. D.H. Buckley & R.L. Johnson, "The Influence of Crystal Structure and Some Properties of Hexagonal Metals on Friction and Adhesion", *Wear*, v.11, pp405-419, (1968).
12. J.H. Lindsay, et. al., "The Interaction Between Electroplated Zinc Deposit Structure and the Forming Properties of Sheet Steel", *Plat. and Surf. Finishing*, v.76, no.3, pp62-69,(1989).
13. J.M. Challen & P.L. Oxley, "An Explanation of the Different Regimes of Friction and Wear Using Asperity Deformation Models", *Wear*, v.53, pp229-243, (1979).
14. C.M. Edwards & J. Halling, "An Analysis of the Plastic Interaction of Surface Asperities and its Relevance to the Value of the Coefficient of Friction", *J. Mech. Eng. Sci.*, v10, pp101-110, (1968).
15. T. Wanheim et. al., "A Theoretically Determined Model for Friction in Metal Working Processes", *Wear*, 28, pp 251-258, (1974).
16. C.S. Barrett & T.B. Massalski, **Structure and Properties of Metals**, 3rd Edition, Pergamon Press, Oxford, p561, (1980).
17. H. Takechi, et. al., "Textures and Properties of Metallic Coatings on Sheet Steels", in ref (8) pp209-222.
18. V. Rangarajan, et. al., "The Effect of Texture and Microstructure on Deformation of Zinc Coatings", *J. Mater. Shap. Tech.*, v.6, pp217-227, (1989).
19. B.D. Cullity, **Elements of X-Ray Diffraction**, 2nd ed., Addison-Wesley, Menlo-Park, CA, (1978).
20. L.G. Schultz, "A Direct Method for Determining Preferred Orientation of a Flat Reflection Sample Using a Geiger Counter X-ray Spectrometer", *J. Appl. Phys.*, v.20, pp1033-1036, (1949).
21. H. R. Wenk, **Preferred Orientation in Deformed Metals and Rocks: An Introduction to Modern Texture Analysis**, Academic Press, (1985).

Textural Characterization and its Applications on Zinc Electroplated Steels

22. M. Hatherley & W. B. Hutchinson, **An introduction to Textures in Metals**, The Institution of Metallurgists, Monograph No. 5.
23. H.D. Nine, "The Applicability of Coulombs's Friction Law to Drawbeads in Sheet Metal Forming", *J. Applied Metalworking*, Vol.2., No.3, (1982).
24. H.D. Nine, "Testing Lubricants For Sheet Metal Forming", *Proc. of The Metallurgical Society of AIME*, St. Louis, MO, (1982).
25. S.-W. Pak, Y. Lin, & M. Meshii, "Effect if the Crystallographic Orientation on Behavior Commercial Zinc Coatings", (Paper Presented at 1989 TMS Fall Meeting, Indianapolis, Indiana, Oct. 2-5).
26. H.D. Nine, "Drawbead Forces in Sheet Metal Forming", in **Mechanics of Sheet Metal Forming**, D.P. Koistinen & N.-M. Wang, eds., Plenum Press, pp 179-211, (1978).
27. R.K.W. Honeycombe, **The Plastic Deformation of Metals**, p114, 2nd Edition, Edward Arnold, London, (1984).

Figure Captions

Figure 1) Schematic representation of results of in-sheet-plane texture measurements. This technique gives the relative amounts of grains with a particular plane parallel to the sheet surface, only between those planes measured, and assumes rotational symmetry (fiber texture) about the sheet normal.

Figure 2) Examples of sharp in-sheet-plane textures from laboratory prepared samples for use in friction and deformation studies. Below are schematic representations of crystals of zinc corresponding to the primary texture components.

Figure 3) Results of calculations of maximum resolved shear stress (RSS) on the basal slip systems for single crystals with three inclinations of the basal plane w.r.t the sheet plane for the range of plane strain loading conditions simple shear ($\alpha=0$) to pure compression ($\alpha=1.0$). RSS exhibits large differences depending crystal rotation about the sheet normal w.r.t. loading direction.

Figure 4) a) Schematic diagram of geometry for Schultz reflection technique for pole figure measurement. b) Stereo-graphic representation for angles corresponding to this geometry.

Figure 5) Basal (002) and prism ($10\bar{1}0$) pole figures of two commercial EG coatings, as deposited (top) and deformed 25% in tension (below). The coating in (a) exhibits little change in texture after deformation, while in (b) slip induced rotation of grains results in changes in position of basal planes both towards sheet normal (moved towards center) and away from tensile axis (lower intensity along N/S direction). Tensile axis is vertical. (Contour spacing is 0.5 mrd, first contour at 1.0 mrd, dots in areas less than 1.0 mrd, equal area projection.)

Figure 6) SEM micrographs of EG coating surfaces corresponding to figure 3. Elongation of coating of commercial sample A was accomplished by intergranular cracking, while coating from sample B deformed by slip, resulting in grain rotation, and remained intact.

Figure 7) Basal pole figures from two commercial (a,b) and three laboratory (c,d,e) EG coatings in the as deposited condition (left) and after drawbead simulation friction testing (right). (a,b,d,e: Contour spacing is 0.5 mrd, first contour at 1.0 mrd, dots in areas less than 1.0 mrd, equal area projection. c: contour spacing is 2.0 mrd for as deposited and 1.0 for DBS tested, equal area projections).

Figure 8) SEM of cross sections of cryogenically fractured of laboratory samples #2 and #3 after friction testing showing apparently shallow depth of deformation. (Steel substrate is at bottom.)

Figure 9) Reduction in intensity of x-ray signal with depth for four different x-ray sources. Depth calculation accounts for in-and-out distance corresponding to 0002 reflection for each tube. Measurement after removal of known coating thickness allows texture as function of depth to be studied.

Figure 10) Evidence of twinning in laboratory deposited, near $11\bar{2}0$ prism oriented specimen. a) As deposited texture, b) texture after strip-drawing. c) Re-measurement after removal of 4 microns of coating shows a return to original texture below that depth.

Schematic Representation of Percentages of Crystallographic Planes Plotted as a Function of Angle of From Basal Plane

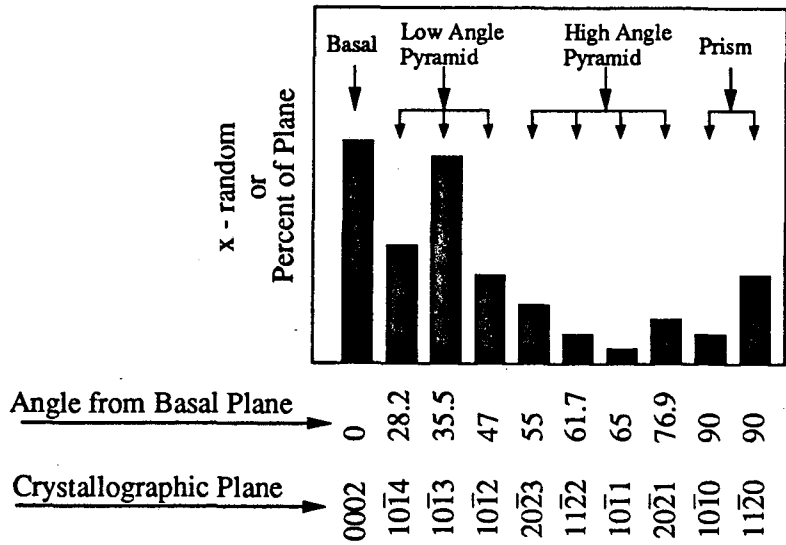


Figure 1

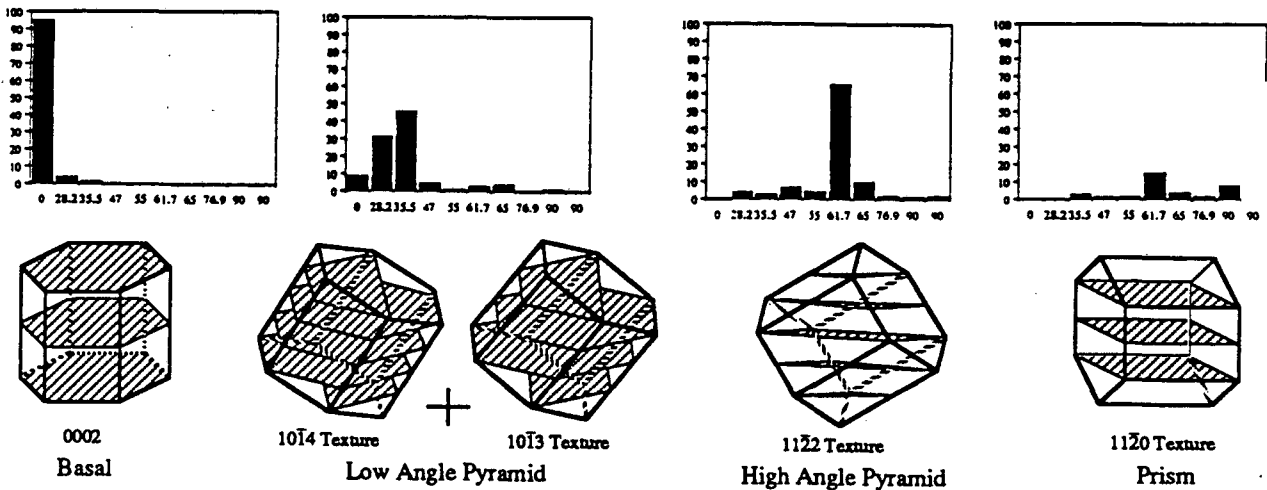


Figure 2

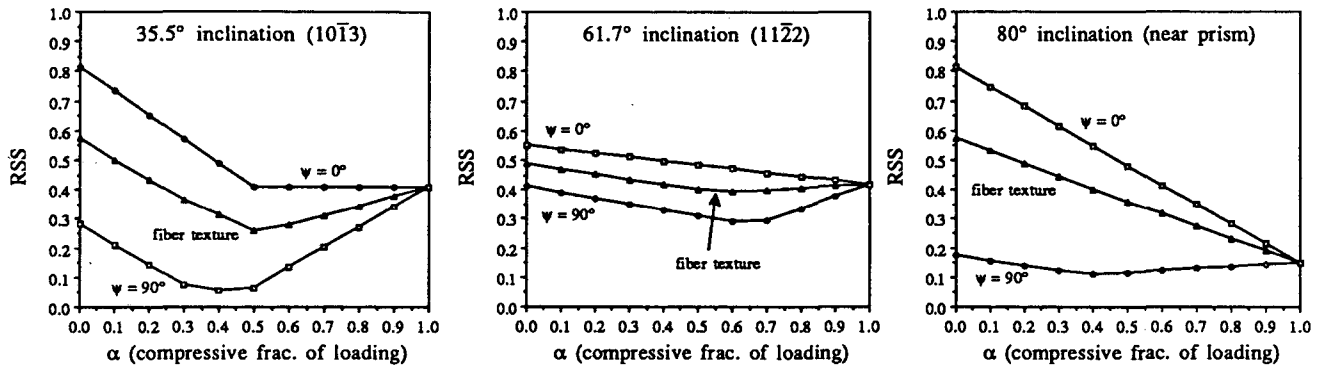


Figure 3

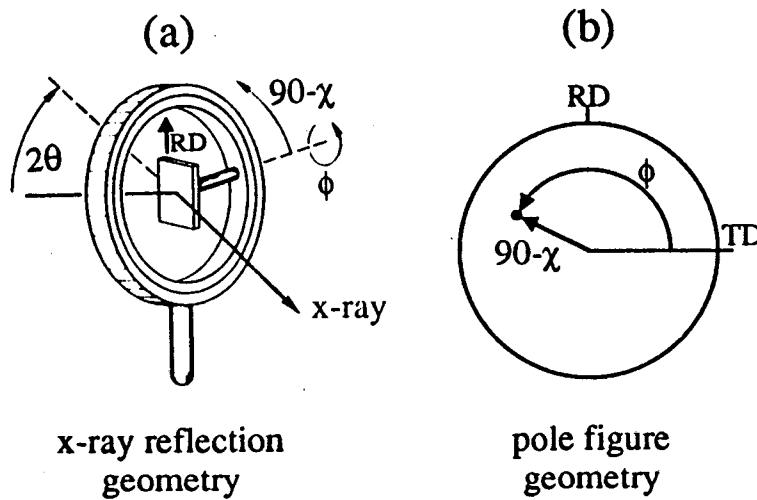


Figure 4

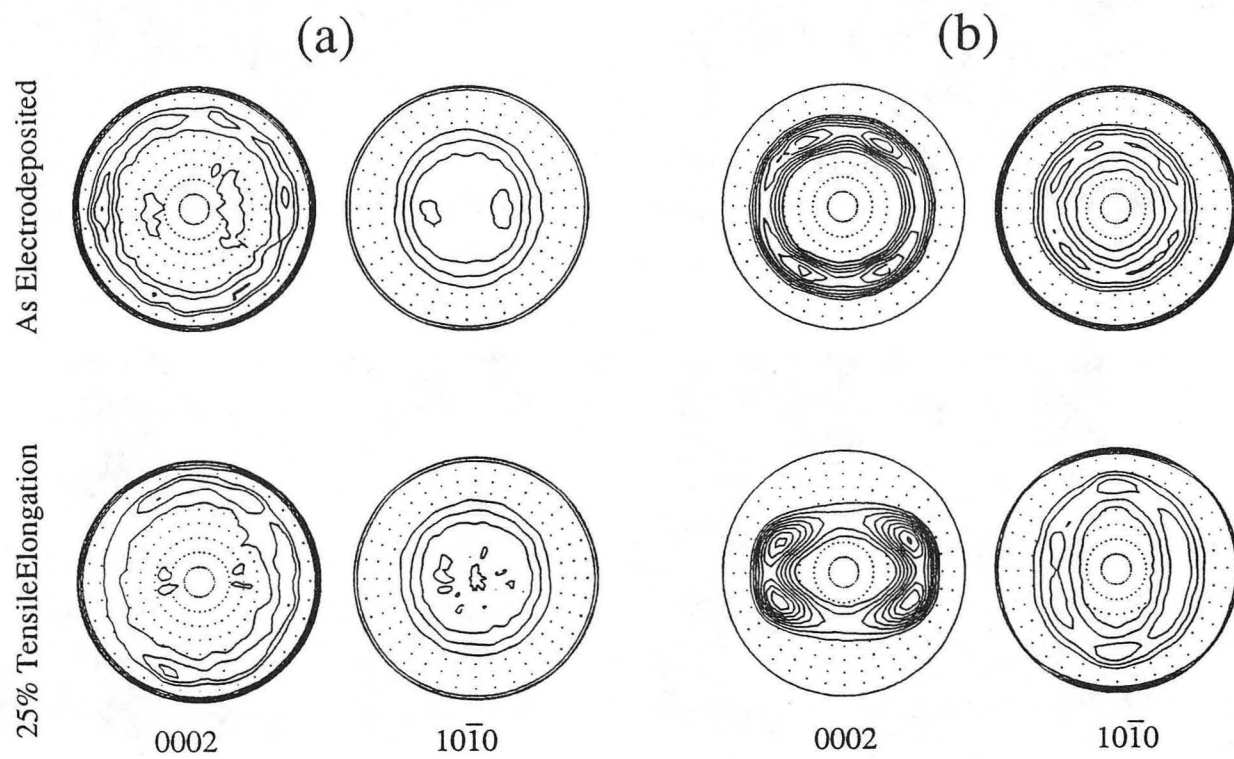


Figure 5

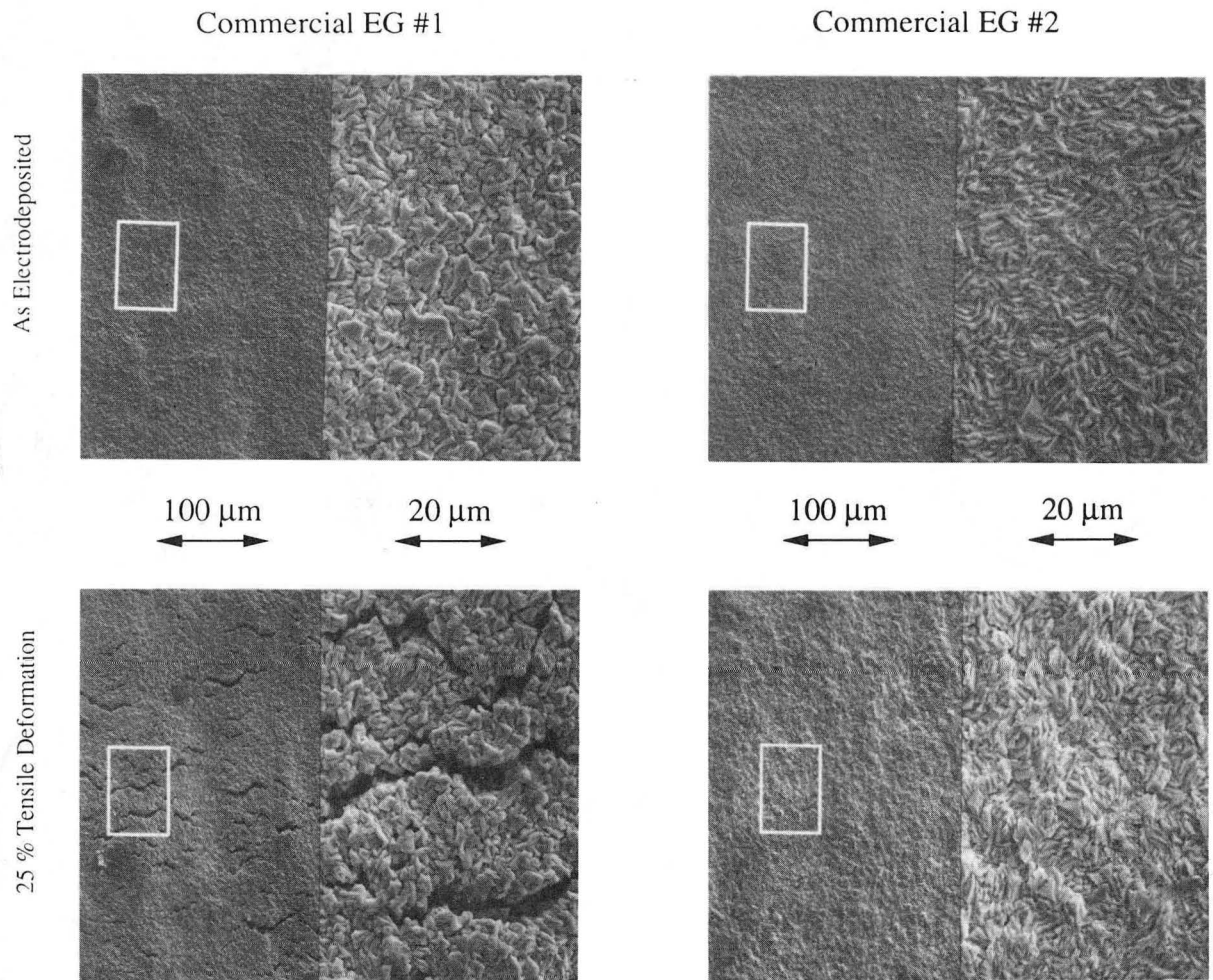


Figure 6

XBB 904-3481

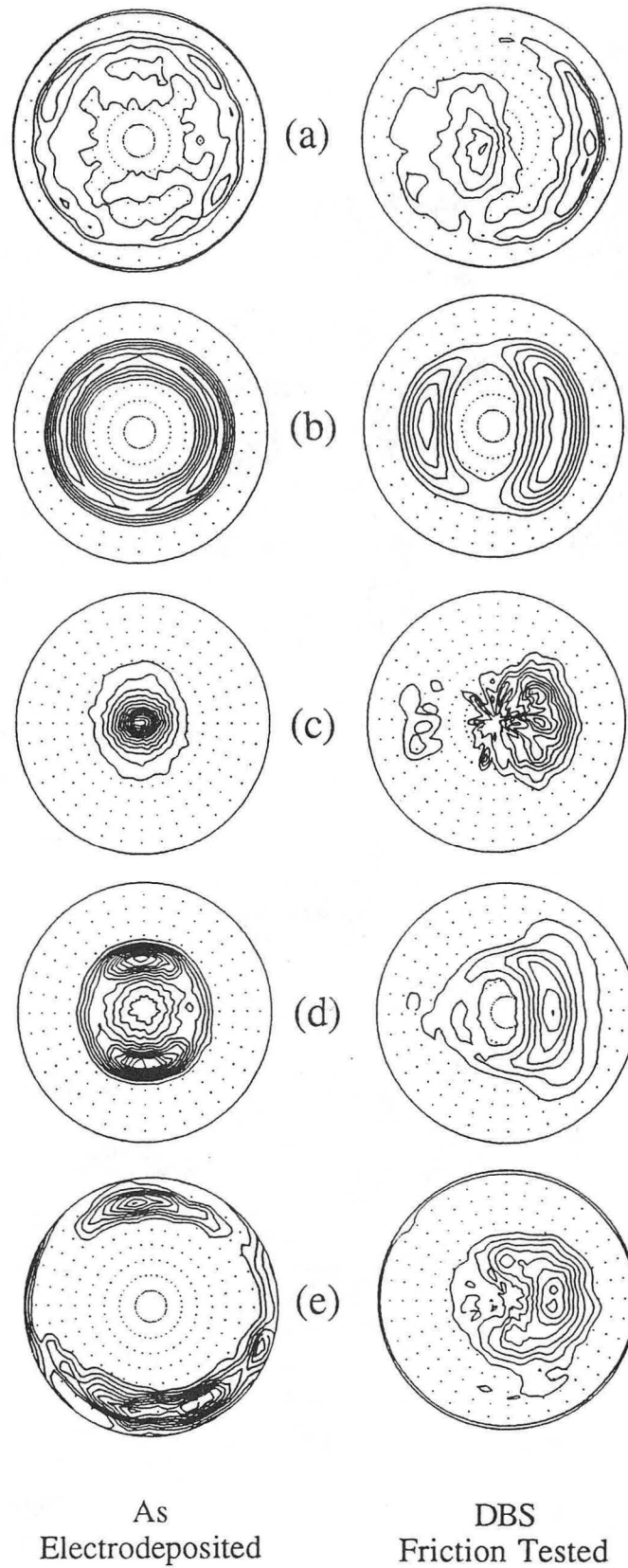


Figure 7

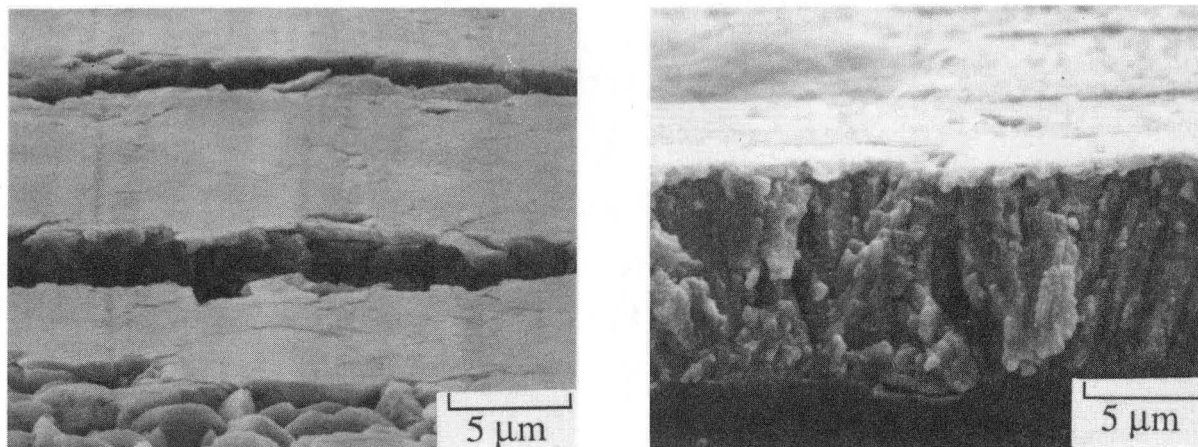


Figure 8

XBB 905-3533

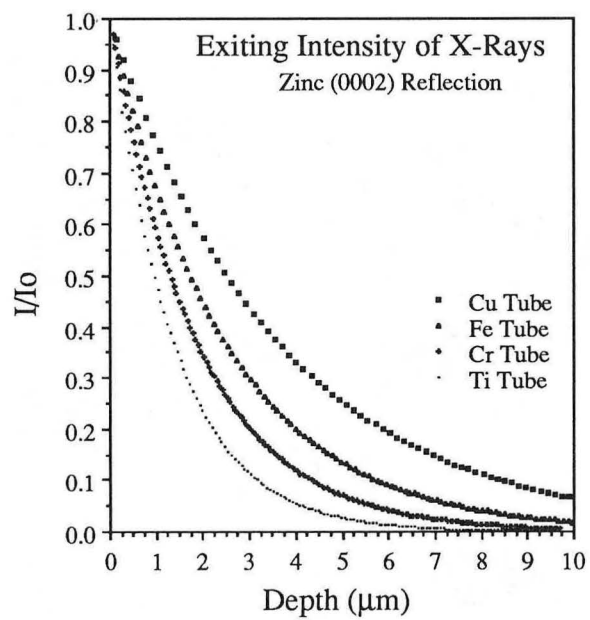


Figure 9

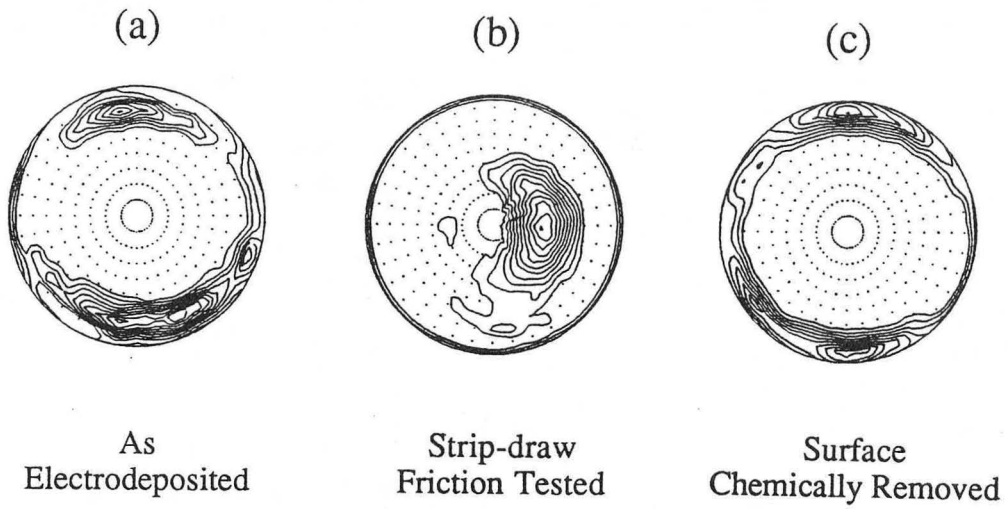


Figure 10

*LAWRENCE BERKELEY LABORATORY
CENTER FOR ADVANCED MATERIALS
1 CYCLOTRON ROAD
BERKELEY, CALIFORNIA 94720*